Agilent
On-Line Analysis of Organic Components in Fine and Ultrafine Particles by Photoionization Aerosol Mass Spectrometry

Authors:
Berk Öktem, Michael P. Tolocka, and Murray V. Johnston
Department of Chemistry and Biochemistry, University of Delaware, Newark, Delaware 19716

A new method, photoionization aerosol mass spectrometry (PIAMS), is described for real-time analysis of organic components in airborne particles below 300 nm in diameter. Particles are focused through an aerodynamic lens assembly into the mass spectrometer where they are collected on a probe in the source region. After a sufficient amount of sample has been collected, the probe is irradiated with a pulsed infrared laser beam to vaporize organic components, which are then softly ionized with coherent vacuum ultraviolet radiation at 118 nm (10.5eV). Since the photon energy is close to the ionization energies of most organic compounds, fragmentation is minimized. Both aliphatic and aromatic compounds of atmospheric relevance are detected and quantified in the low- to midpicogram range. The photoionization signal intensity increases linearly with the amount of material sampled and is independent of particle size. The fragmentation induced by laser desorption is greater than that observed with thermal vaporization, suggesting that the internal energy imparted by the former is greater. Although some molecular fragmentation is observed, mass spectra from common sources of ambient organic aerosol are distinguishable and consistent with previous off-line measurements by gas chromatography/ mass spectro-metry. These results illustrate the potential of PIAMS formolecular characterization of organic aerosols in ambient and smog chamber measurements.

The organic fraction of urban airborne particulate matter is a complex mixture of compounds with a combined concentration on the order of 1-12 µg/m^3, accounting for up to 54% of the total fine particle mass (particles less than 2.5 µm in diameter). Major compound classes and their typical mass concentrations in urban aerosol include aliphatic hydrocarbons (55 ng/m^3), organic acids (500 ng/m^3), and polycyclic aromatic hydrocarbons (PAHs; 10 ng/m^3). For individual compounds, the mass concentrations are usually 10 ng/m^3 or less. These concentration levels present ananalytical challenge: identification and analysis of individual organic components in ambient aerosol require long sampling times and laborious sample cleanup and analysis. Measuring these small amounts of material involves a typical sampling duration of 12-24 h, which makes it difficult to follow changes in the physicochemical properties of an aerosol on short time scales. Information of this type is needed to understand atmospheric chemical processes such as the formation and subsequent reactivity of secondary aerosols.

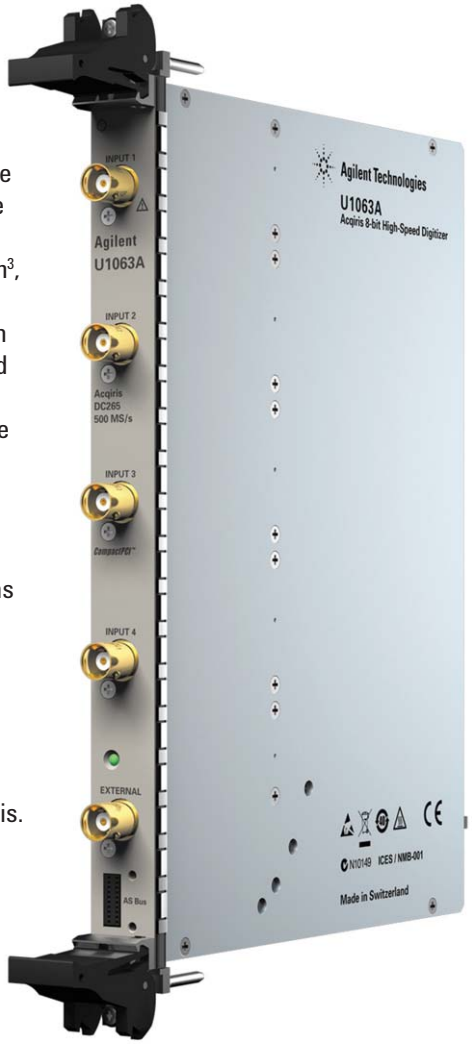

Figure 1. Agilent Acqiris U1063A cPCI digitizer card

Single-particle mass spectrometers provide valuable data on the chemical composition of ambient particulate matter in real time. Individual particles are drawn into the mass spectrometer and ablated by a pulsed, ultraviolet laser beam typically at 193 or 266 nm. Ions formed by the ablation event are then analyzed by time-of-flight mass spectrometry. The mass spectrum of an individual particle provides a chemical signature that can be related to its source or transformation in the atmosphere. Chemical signatures are readily obtained from inorganic components such as metals, nitrate, and sulfate. Organic and elemental carbon can also be detected, but the ablation/ionization process is usually too harsh to preserve structural information from individual organic compounds. To address this issue, two-step laser desorption/ionization methods have been developed for single particles, but limitations remain.

Two-step laser desorption/ionization has been extensively studied as a means of characterizing samples immobilized on a substrate. For example, Hahn et al. demonstrated subfemtomole quantitation of immobilized samples containing aromatic chromophores by infrared laser desorption followed by resonance twophoton ionization (R2PI) with an ultraviolet laser. This approach was subsequently adapted to characterize particulate matter on filters and has been applied to different types of samples including ambient organic aerosols, tobacco smoke, and PAHs. For PAHs, subnanogram detection limits and quantitation over 2 orders of magnitude were achieved. R2PI provides high sensitivity for detection of aromatic compounds but is not amenable to aliphatic compounds.

Single-photon ionization (SPI) with coherent vacuum ultraviolet (VUV) radiation is suitable for both aliphatic and aromatic compounds. SPI gives little or no fragmentation because the radiation typically used (118 nm, 10.5 eV) is just above the ionization energies of most organic compounds. Baer and coworkers have employed SPI for real-time detection of molecules desorbed from individual particles with an infrared laser pulse. Both quantitative detection and depth profiling of organic components in single particles have been demonstrated. This group has also employed a setup where individual particles are detected by light scattering and vaporized by impacting a heated probe and the organic components characterized by SPI. Prather and co-workers have used R2PI to detect aromatic species desorbed from individual particles by an infrared laser pulse. In all of these experiments, individual particles smaller than ~1 μm in diameter are difficult to analyze because the ion signal becomes vanishingly small. This is a problem for ambient measurements since most organic matter exists in much smaller particles.

An approach for on-line characterization of organic compounds in "bulk" samples containing particles smaller than 1 μm has been reported by Tobias and Ziemann and later by Jayne and co-workers. In each case, particles enter the mass spectrometer through an aerodynamic lens assembly that efficiently transmits fine particles and focuses them into a tight beam. The particle beam impacts a heated probe where organic (and semivolatile inorganic) components are vaporized and then ionized by 70-eV electron ionization (EI) in a quadrupole mass spectrometer. Good sensitivity is achieved for particle sizes down to several tens of nanometers in diameter by integrating the signal over a large number of particles. Particles may also be collected on a cooled probe where a temperature-programmed heater is used to for vaporization. Temperature programming helps to separate and identify compounds based on their volatilities. Particle size can be determined by inserting a mechanical chopper in the particle beam path and measuring the transit time between the chopper and mass analyzer. Quantitative measurements are also possible. The main limitation of this approach is that 70-eV EI can cause extensive fragmentation, making it difficult to detect molecular ions, particularly for aliphatic compounds.

A thermal desorption/chemical ionization mass spectrometer has been described recently by Voisin et al. for analysis of particles in the low-nanometer size range. Charged particles are electrostatically collected on a probe that is subsequently inserted into the mass spectrometer for analysis. This method has been used to characterize inorganic materials such as ammonium sulfate particles and may also be applicable to organic compounds.

In the work described here, a first-generation field-deployable photoionization aerosol mass spectrometer (PIAMS) is described for analysis of particles down to several tens of nanometers in diameter. Particles enter the mass spectrometer through an aerodynamic lens assembly and deposit on a probe surface. The probe is irradiated with a 1064-nm Nd:YAG laser, and the vaporized molecules are photoionized with coherent VUV radiation at 10.5 eV. Relative to existing methods for fine and ultrafine particle analysis based on 70-eV EI, this approach is found to give less fragmentation and higher sensitivity for molecular ion detection. The application of this method to characterization of organic aerosols is discussed.

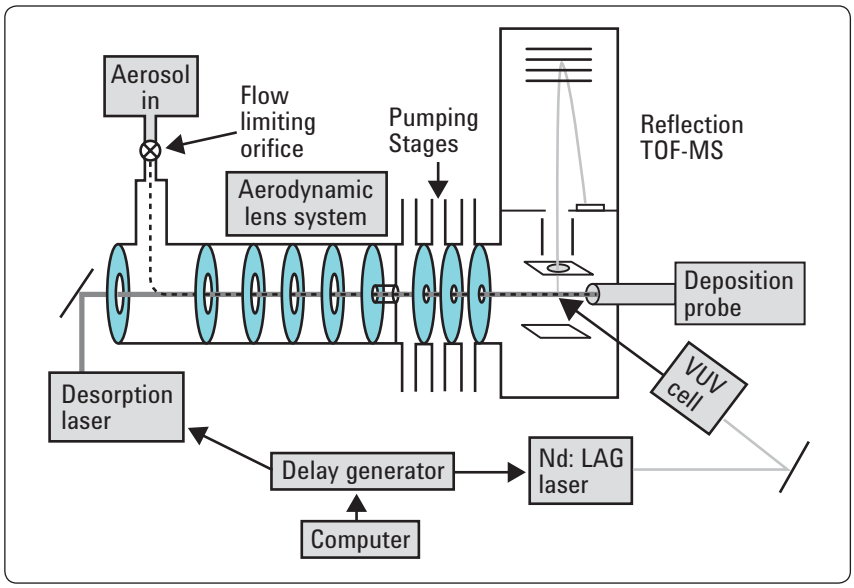

Figure 2. Schematic of the photoionization aerosol mass spectrometer (PIAMS).

Experimental Section

The PIAMS is shown schematically in Figure 1. The mass spectrometer consists of a particle inlet, collection probe, vacuum ultraviolet conversion cell, and reflectron time-of-flight mass analyzer, all mounted on a 6-in. cube. The lasers, optics, mass spectrometer, Acqiris digitizer system, and associated electronics fit on a 31 in. by 48 in. cart. Automated operation of the instrument is performed with software developed from LabVIEW (National Instruments, Austin, TX).

Aerosols are sampled into the mass spectrometer through a flow-limiting sapphire orifice with a 110-µm diameter (O'Keefe Controls Co., Monroe, CT) giving a volume flow rate of 0.09 L/min and an inlet pressure of 1.8 Torr. In the reduced pressure region, particles are focused into a tight beam in the center of the gas flow with an aerodynamic lens system. After exiting the lens system, the particle beam is selectively transmitted into the mass spectrometer source region through three differentially pumped stages. The stages are separated by 2-mm-diameter, 12-mm-long capillaries mounted 10 mm below the exit of the previous stage. The surface at the inlet end of each capillary has a conical shape to increase pumping speed. The wide diameter of these capillaries facilitates passing the desorption laser beam through them without sacrificing particle transmission efficiency relative to that reported previously. It should be noted that particle transmission is dependent upon particle shape and hence composition. Spherical particles are focused into a tight beam while nonspherical particles are subject to additional lift forces that degrade aerodynamic focusing. While the particle beam exiting the lens assembly does diverge, the transit distance to the collection probe is short and the beam diameter remains less than 1 mm wide.

The collection probe is a flat cylindrical rod (3-mm diameter) made of aluminum. It is located within the mass spectrometer source volume 8 mm from the center of the source region and kept at a constant potential close to the average value of the potentials applied to the source plates. A Nd:YAG laser (Minilite II, Continuum, Santa Clara, CA) operated at 1064 nm (5-ns pulse) is used to desorb molecules from particles that are deposited on the probe. As shown in Figure 1, the desorption laser beam enters the mass spectrometer collinear with the particle beam. The center portion of the beam from the laser is directed onto the probe surface without any focusing optics. With this configuration, ~ 30% of the radiation leaving the laser strikes the probe surface. The entire probe surface is illuminated, but not evenly. No attemptwas made to measure the laser beam profile across the probe surface. In most experiments, the desorption laser pulse energy was set to 23 mJ.

In some experiments, a compact carbon dioxide laser with 10.6-µm wavelength (µ-TEA 10.6, Laser Science Inc., Franklin, MA) was used for desorption. However, all of the results reported here were obtained with the Nd:YAG laser as higher signal levels were uniformly obtained. Two other experimental arrangements were studied as a means to vaporize the sample. First, a heated probe was used to flash vaporize particles impinging on the probe. Second, off-line analysis of bulk samples was performed by placing the sample in a direct insertion probe and heating until molecular evaporation occurred. While useful for studying the characteristics of particle vaporization, these thermal desorption methods are not as useful for practical applications because most of the vaporized sample traverses the source region while the photoionization laser is off.

The plume of molecules formed during the desorption step travels back to the center of the source region where it is irradiated with a pulse of coherent VUV radiation at 118 nm (10.5eV) generated by a second Nd:YAG laser (Tempest 10, New Wave Research, Fremont, CA) at 355 nm. VUV radiation is produced by nonresonant frequency tripling in a xenon-argon mixture (8.5% xenon in argon; total pressure 185 Torr). Typically, a 37 mJ pulse at 355 nm is focused into the gas cell (20 cm long) with a 15-cm f.l. lens. The VUV radiation is refocused in the mass spectrometer source region with a MgF2 lens (5.9 cm f.l. at 118 nm). This lens does not refocus the residual 355-nm radiation. Although the 118-nm and residual 355-nm beams are collinear, the 355-nm beam has

little apparent effect on ionization/fragmentation since its size is large facilitates passing the desorption laser beam and its irradiance is low. The VUV pulse energy is not measured, but it is expected to be on the order of 1-2 µJ based on our previous work. Ions produced by the VUV pulse are analyzed with a reflectron time-of-flight mass analyzer (R. M. Jordan Co., Grass Valley, CA).

A delay generator (DG535, Stanford Research Systems, Sunnyvale, CA) synchronizes the desorption and ionization lasers by generating Q-switch pulses for each with an appropriate time delay, typically on the order of 30 Ìs. The delay generator also triggers a high-voltage pulser (model GRX 1.5K-E, Directed Energy Inc., Fort Collins, CO) so that the potential of a deflector plate in the mass analyzer, which steers the ions through the reflectron assembly, is pulsed coincident with the VUV pulse. The delay time of this pulse can be adjusted to reject ions from the desorption laser pulse or low-m/z ions produce produced by the VUV pulse, as needed. During the particle collection and desorption steps, the two source plates and collection probe are held at ground. These potentials are raised to their proper values for ion extraction shortly before the VUV laser fires. This combination provides additional rejection of ions produced by the desorption laser beam. The ion current from the detector is measured with a 500-MHz digitizer (Agilent Acqiris U1063A digitizer with U1091A crate). Two channels with 8-bit resolution are simultaneously recorded with different sensitivities and then recombined into one spectrum by the software to increase the dynamic range of detection.

For the work described here, polydisperse aerosols were generated with a constant-output atomizer (model 3076, TSI Inc., St. Paul, MN). In all cases, particles were generated from a solution containing 0.1 g of analyte in 500 mL of ethanol. All chemicals were purchased from Sigma-Aldrich (St. Louis, MO). Monodisperse aerosols were generated by size selecting this aerosol stream through a differential mobility analyzer (model 3085, TSI Inc.). The particle number density was measured by a condensation particle counter (model 3025 A, TSI Inc.).

In most experiments, sampling was done in a "batch" mode where the inlet valve controlling the particle flow was opened for a set period of time. During the sampling period, particles deposited on the probe and the lasers were inactive. After the inlet valve was closed, the desorption and ionization lasers were fired at 10 Hz to obtain a spectrum. The number of laser shots required to completely remove the collected material (i.e., bring the ion signal down to the background level) depended on the desorption laser pulse energy. For a pulse energy of 23 mJ from the desorption laser, 150 shots were typically required. A few experiments were performed in a "continuous" mode in which the desorption and ionization lasers were fired at a variable repetition rate (1-10 Hz) while the inlet valve was open. After the inlet valve was closed, the repetition rate was set to 8 Hz and the lasers continued to fire until all of the collected material was removed. The continuous mode permitted the effect of the desorption laser on particles flowing through the aerodynamic lens system to be studied.

Source sampling was performed with stainless steel canisters having a nominal volume of 6 L (SKC Inc., Eighty Four, PA). The canisters were evacuated to less than 0.1 Torr, transported to the sampling site, and then opened to admit the ambient aerosol (80 s at a flow rate of 5 L/min). After sampling, the canisters were returned to the laboratory and analyzed within 10-15 min of obtaining a sample.

Results and Discussion

Particle Sampling. Particle sampling into the PIAMS is a twostep process: transmission through an aerodynamic inlet that bridges atmospheric pressure and the high-vacuum environment of the mass spectrometer, and collection on a probe. As described in the Experimental Section, the aerodynamic inlet assembly is designed to focus a broad range of particle sizes into a tight beam while at the same time providing a wide aperture through which the desorption laser beam can pass. Since the particle and laser beams are collinear, it is possible that some particles are irradiated by the desorption laser pulse while traveling through the inlet. If this occurs, then some analyte may be prematurely vaporized and never reach the collection probe. Fortunately, the transit time of particles in the desorption laser beam path is short. For example, 150-nm-diameter particles are expected to spend on the order of 12 ms in the aerodynamic inlet assembly and less than 1 ms in transit from the inlet to the collection probe. These values are based on the gas flow rate in the aerodynamic lens assembly and the expected velocity of particles in the vacuum.

Premature vaporization of the analyte by the desorption laserpulse was studied experimentally by comparing the "continuous" and "batch" modes of sampling (see Experimental Section) for 150-nm-diameter oleic acid particles with a 1-min collection period (500 pg sampled). Oleic acid was chosen because it forms spherical particles that focus into a tight particle beam within the desorption laser beam path. As expected, firing the desorption laser in the 1-10-Hz range during sampling did not decrease the photoionization signal. In fact, the signal was enhanced over that obtained with the batch mode by up to a factor of 3, with higher repetition rates during the sampling period generally giving higher signal levels. The higher signal levels with the continuous mode of operation most likely arise from the shorter sampling/analysis time, which reduces the amount of sample evaporation from the probe (see Fligure 2, page 5).

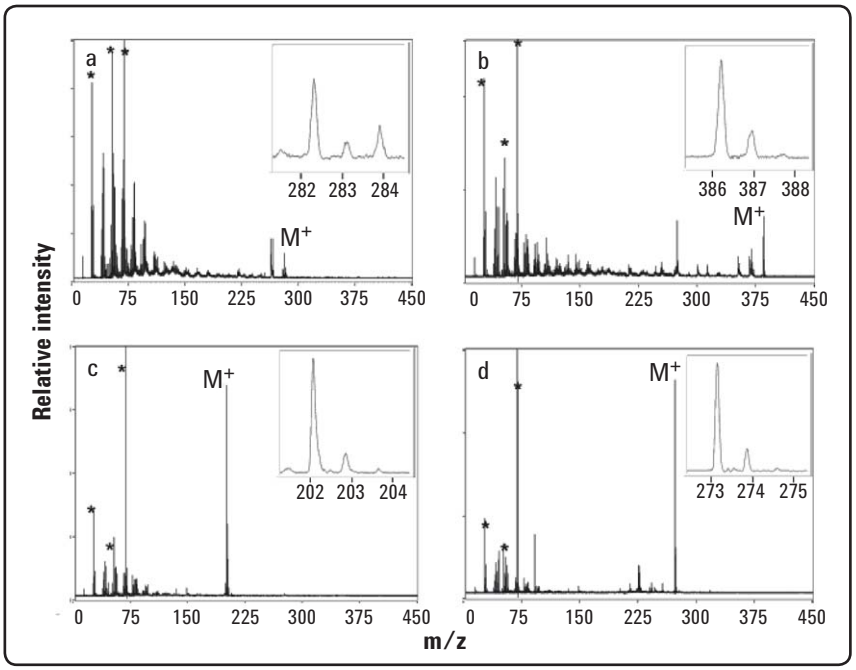

Figure 3. PIAMS spectra of (a) oleic acid, (b) cholesterol, (c) pyrene, and (d) 6-nitrochrysene. Peaks marked with an asterisk denote ions from probe material. The enhanced signal at 284 m/z in the oleic acid mass spectrum is from stearic acid impurity.

Particles striking the collection probe do not necessarily deposit and remain on the probe until analysis. Sample may be lost if particles bounce off the surface after impact or if evaporation occurs after particles are collected. Particle bounce occurs when the rebound energy is greater than the adhesion force. Although the experimental apparatus does not allow particle bounce to be measured, it is likely that bounce occurs since the size-dependent particle velocities from the inlet exceed the critical velocities required for sticking to a metal surface.Particle bounce can be minimized by coating the surface with a sticky substance, modifying the probe geometry, or both. Coating the probe surface is not relevant to PIAMS because the probe resides in a high vacuum and background signal must be minimized.

The probe geometry used in this work, though nominally flat, contained a microscopically roughened (i.e., unpolished) surface. This geometry may facilitate particle capture by increasing the probability that a particle recoiling from the initial impact strikes another portion of the surface and sticks.

A conical probe geometry similar to that described by Ziemann and co-workers was investigated as an alternative way to collect recoiling particles. Unfortunately, the conical geometry gave very low signal levels, presumably because the surface reflected and focused the desorption laser beam, making simple molecular vaporization less favorable than ablation, ionization, and fragmentation.

Sample evaporation off the probe was found to significantly influence signal levels. The effect of evaporation during sampling was studied with the "batch" mode of operation by introducing the same total particle mass over varying periods of time. A relatively volatile compound, pyrene, was chosen for this experiment. Pyrene particles, 150 nm in diameter, were generated at different number concentrations (particles/cm3) such that the same total mass of analyte (500 pg) could be sampled over time periods between 20 and 320 s. The photoionization signal intensity remained constant when the sample was deposited over a time period up to 60 s. Longer sampling periods resulted in significantly lower signal intensities. In another series of experiments, a constant amount of oleic acid (150-nm-diameter particles, 500 pg of total mass) was sampled over a period of 1 min, and the delay time between sampling and analysis was varied. Oleic acid is less volatile than pyrene but it still may evaporate and, as it exists in liquid form, may flow off the probe. It was found that delaying the analysis 30 s or longer after sampling resulted in a significantly decreased signal level. To minimize evaporation in subsequent experiments, sampling times of 1 min or less were used with no time delay between sampling and analysis.

The particle size dependence of the sampling and collection steps was investigated by sampling particles of different sizes but with the same total amount of oleic acid sampled (500 pg) and the same sampling time (1 min). The photoionization signal intensity was found to be independent of particle size between 80 and 250 nm. Particles smaller than 80 nm could be size selected and sampled, but more than 1 min was required to sample 500 pg and evaporation compromised the results. Particles larger than 250 nm could not be generated and size-selected with the available instrumentation.

Particle Vaporization. Since the particles used in this study are relatively transparent at the desorption laser wavelength (1064 nm), the dominant mechanism of analyte vaporization is thought to be fast heating of the metal surface followed by heat transfer to the collected particle from which the analyte desorbs. Heat transfer to the particle competes with surface cooling by diffusion into the bulk. Typically, surface heating rates exceed 1010 K/s during the laser pulse, while cooling after the laser pulse occurs on the time scale of 1 µs or less. When a constant amount of oleic acid is sampled into the PIAMS (150-nm-diameter particles, 500 pg sampled), the molecular ion ($M^{\bullet+}$, 282 m/z) signal intensity initially increases with increasing desorption

laser pulse energy, reaches a maximum, and then decreases as the desorption laser pulse energy increases further. The maximum molecular ion signal is obtained with a pulse energy of 23 mJ from the desorption laser, which corresponds to an irradiance of ~0.1 J/cm2 (40 MW/cm2 peak) at the probe surface.

Figure 2a shows the mass spectrum of oleic acid obtained with this laser pulse energy. In addition to the molecular ion, high-m/z fragment ions due to the loss of OH, H_2O, and C_3H_6O from the molecular ion (265, 264, and 222 m/z, respectively), fragment/background ions of the type C_xHy^+, and substrate ions (Al^+, Al_2^+, and Al_2O^+ at 27, 54, and 70 m/z, respectively) are observed.

The initial increase of molecular ion signal intensity with increasing desorption pulse energy reflects the higher probability for oleic acid vaporization as the surface temperature increases. Above the optimum pulse energy, the molecular ion intensity decreases relative to the fragment ions, and both the fragment and molecular ions decrease relative to the substrate ions. In addition, large amounts of Al^+ are formed directly by the desorption laser pulse, suggesting that one-step ablation/ionization becomes a dominant mechanism. It is also found that the number of laser shots required to completely vaporize the analyte (i.e., bring the analyte signal down to the background level) decreases as the pulse energy increases.

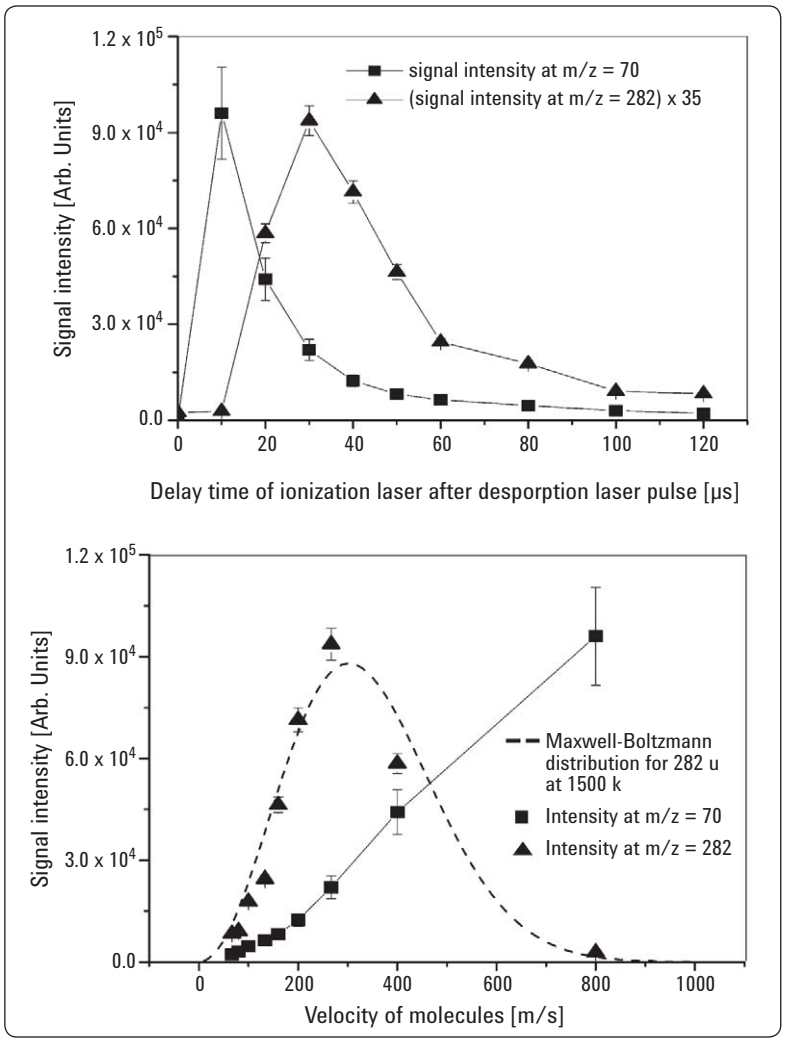

Figure 4. (a) Signal intensity vs delay time between the desorption and photoionization pulses for 70 (probe material) and 282 m/ z(oleic acid). (b) signal intensity vs velocity of neutral precursors to 70 and 282 m/ z. The dashed line in (b) represents the best fit to a Maxwell- Boltzmann velocity distribution (1500 (100 K for 282 u). The solid lines in (a) and (b) are drawn as an aid to the eye.

Further insight into the vaporization process can be obtained from the dependence of the ion signal intensity on delay time between the desorption and photoionization laser pulses. Figure 3a shows how the signal intensities of the molecular ion (282 m/z) and substrate ion (70 m/z) change as a function of delay time. The substrate ion signal reaches a maximum signal intensity at 10 µs corresponding to a most probable velocity from the surface of 800 m/s. The oleic acid molecular ion reaches a maximum signal intensity at a much longer time, 30 µs, corresponding to a most probable velocity of 270 m/s. The different velocities (and kinetic energies) suggest different vaporization mechanisms for the analyte and substrate neutrals. Substrate neutrals are ejected with a higher kinetic energy, suggesting an explosive, ablation process rather than a thermal process. Support for this interpretation is shown in Figure 3b where signal intensity is plotted versus velocity. The velocity distribution of the oleic acid molecular ion roughly fits a Maxwell-Boltzmann distribution with a translational temperature of 1500 ± 100 K (r^2=0.92). The velocity distribution of the substrate ion does not fit a Maxwell-Boltzmann distribution ($r^2 < 0.6$). The translational temperature of vaporized oleic acid is within the range of translational temperatures measured for infrared laser desorption-VUV photoionization of single ethylene glycol particles in the micrometer size range but is somewhat greater than the temperature jump expected for laser heating of metal surface. This observation suggests that some molecules are accelerated by an additional mechanism as they leave the surface, for example, a supersonic expansion.

The velocity distribution in Figure 3b suggests that ~20% of the kinetic energy distribution of molecules desorbed from the probe is intercepted by the VUV pulse, assuming a VUV beam diameter of 200 İm.

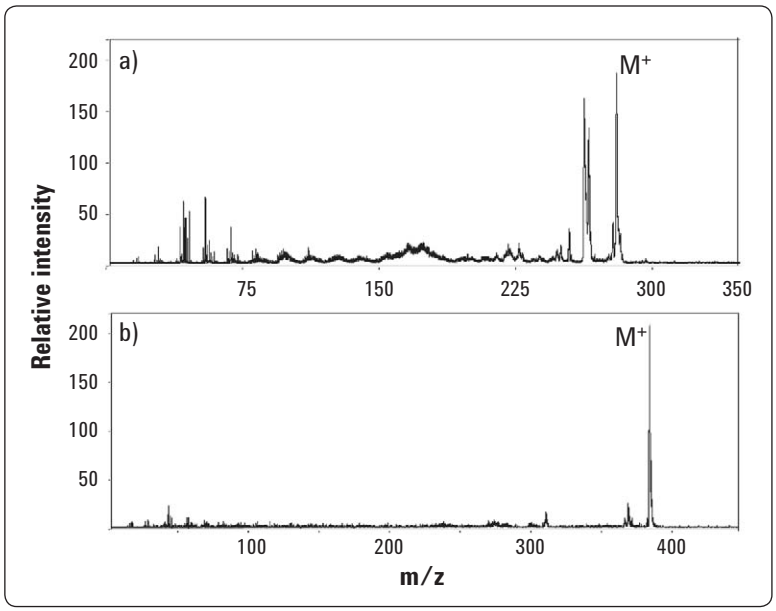

Figure 5. Photoionization mass spectra of (a) oleic acid and (b) cholesterol off a heated direct insertion probe.

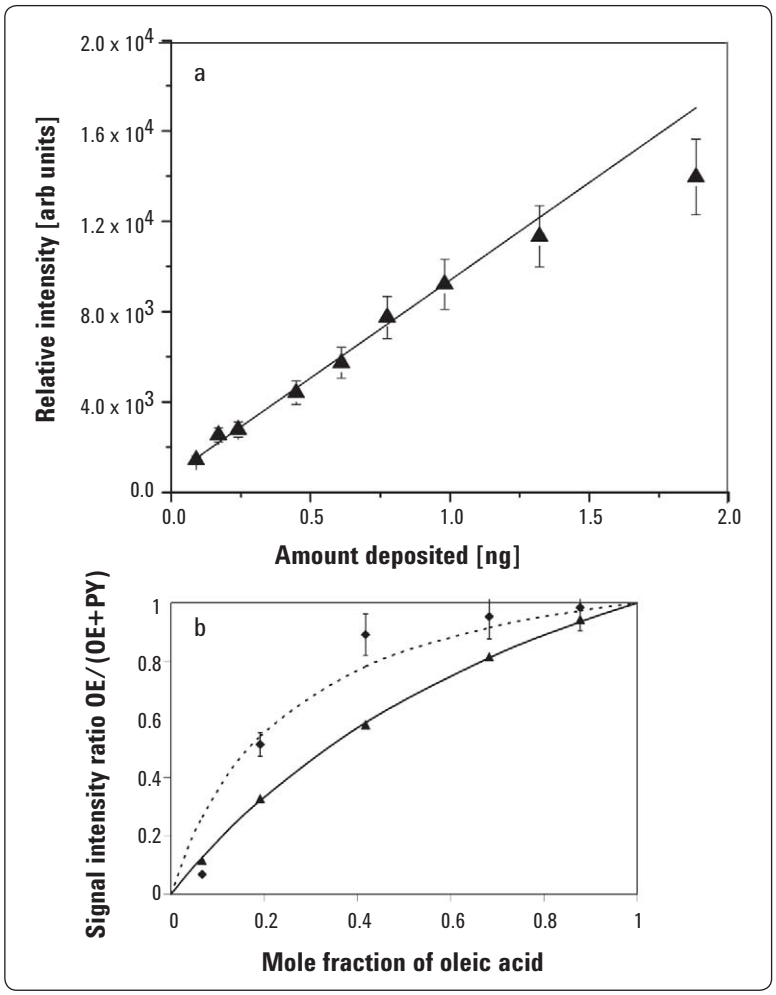

Figure 6. (a) Signal intensity vs mass of oleic acid sampled into the inlet. Error bars represent one standard deviation. (b) Signal intensity ratio of oleic acid (264 + 282 m/ z) to the sum of oleic acid and pyrene (202 + 203 + 264 + 282 m/ z) vs mole fraction of oleic acid for thermal (Δ) and laser (♦) desorption of aerosol particles. Solid curve is the expected plot for a relative sensitivity 2.0; dashed curve is the expected plot for a relative sensitivity of 5.0.

Molecular Identification and Quantification. Representative laser desorption photoionization mass spectra of four atmospherically relevant compounds are shown in Figure 2. The spectrum of oleic acid in Figure 2a has already been discussed in part. Oleic acid in the troposphere is a product of vegetative burn with an annual average concentration of 25 ng/m^3 under ambient conditions. The signal-to-noise ratio (SNR) of the molecular ion in Figure 2a is 46, suggesting a detection limit (SNR = 3) for oleic acid of 35 pg sampled through the inlet. When oleic acid aerosols are analyzed by thermal desorption with 70-eV EI, the molecular ion intensity is very small, ~0.01% of the base peak in the spectrum. In contrast, the molecular ion signal intensity is much greater in Figure 2a, ~30% of the base peak (from oleic acid) at 55 m/z. The molecular ion signal is still not as great as that observed by laser desorption/VUV photoionization of individual microparticles where molecular ion signal is roughly 80% of the base peak at 264 m/z (H2O loss from the molecular ion) and lowmass fragment ions are relatively weak. Figure 4a shows the photoionization mass spectrum of a bulk oleic acid sample vaporized from a direct insertion probe at 150 °C. Much less fragmentation is observed with thermal desorption than with laser desorption, suggesting that the internal energy imparted by the latter is much greater. The broad features in Figure 4a arise from metastable decomposition of the molecular ion. These features are observed with laser desorption, though with less intensity since the internal energy is higher.

Figure 2b shows the laser desorption/photoionization mass spectrum of cholesterol (150-nm particles; 3.3 ng sampled). Cholesterol is found at 2 ng/m^3 in ambient air and is used as a source tracer for meat cooking. In addition to the molecular ion, high-mass fragment ions are observed at 368, 353, 313, 275, and 255 m/z. When a bulk cholesterol sample is vaporized from a direct insertion probe at 180 °C, the spectrum

in Figure 4b is obtained. As with oleic acid, much less fragmentation is observed for cholesterol with thermal desorption than laser desorption. The only significant fragment ion with thermal desorption is 368 m/z, which corresponds to the loss of water. The signal-to-noise ratio of the molecular ion in Figure 2b is 66, suggesting a detection limit of 150 pg provided that the large amount sampled (3.3 ng) is in the linear portion of the calibration plot (see discussion below).

Figure 2c shows the laser desorption/photoionization mass spectrum of pyrene (150-nm particles, 470 pg sampled). Pyrene is one of many polycyclic aromatic hydrocarbons found in ambient air that are known toxicants.5 The molecular ion is observed with little fragmentationsthe low-m/z ions observed in this figure also appear in a sample blank and arise from the probe material and background. The signal-to-noise ratio of the molecular ion is 260, suggesting a detection limit of 5 pg sampled.

Figure 2d shows the laser desorption/photoionization mass spectrum of 6-nitrochrysene (150-nm particles, 450 pg sampled). Nitropolycyclic aromatic hydrocarbons are highly toxic and are released into ambient air through either direct emission or secondary reactions in the atmosphere. The spectrum in Figure 2d is dominated by the molecular ion and a fragment ion at 226 m/z (loss of nitro group). Low-m/z ions are from the probe material and background. Similar fragmentation has been observed in a previous laser desorption resonant two photon ionization experiment. The signal-to-noise ratio of the molecular ion in Figure 3d is 190, suggesting a detection limit of 7 pg sampled.

An important attribute of VUV photoionization is molecular quantification. Since the photoionization energy (wavelength) is fixed, the amount of molecular fragmentation is relatively invariant for a given vaporization method and ion signal intensities are reproducible. The quantitative ability of PIAMS is illustrated in Figure 5. Figure 5a shows the relationship between ion signal intensity (sum of 282 and 264 m/z) and amount of oleic acid sampled. In this experiment, the particle size and number concentration were held constant. Different amounts of oleic acid were sampled by varying the sampling time. Between 90 pg and 1 ng sampled (4-60-s sampling time), a linear relationship is observed. Above 1 ng, the plot flattens out, presumably because evaporation becomes significant as the sampling period exceeds 1 min (see discussion above). It should be noted that if the 150- nm-diameter oleic acid droplets remain intact, only 1% of the probe surface will be covered when 1 ng is deposited on the probe. If the droplets coalesce and spread out evenly over the surface, the coverage will be on the order of two monolayers. The detection limit (SNR) 3) of oleic acid determined from Figure 5a is 30 pg. This is comparable to the detection limit estimated from the molecular ion signal-to-noise ratio in Figure 2a.

Relative quantification of individual components in a binary mixture of oleic acid and pyrene is illustrated in Figure 5b. Two sets of data are shown: analyte vaporization by laser desorption of particles collected on the probe and thermal desorption of particles impacting a heated probe at 650 °C. In the laser desorption experiment, the mole ratio of the two components was varied while the particle size (150 nm) and total amount sampled (500 pg) remained constant. In the thermal desorption experiment, a polydisperse aerosol (50-200-nm diameter) with a much larger total amount sampled (microgram level) was analyzed owing to the lower duty factor of molecular detection. In either case, relative quantification with an uncertainty of (8% was achieved over 2 orders of magnitude in relative concentration. Figure 4b shows plots of the signal intensity ratio of oleic acid (sum of signals at 264 + 282 m/z) to the sum of oleic acid and pyrene (sum of signals at 202 + 203 + 264 + 282 m/z) versus mole fraction of oleic acid in the particles. The relative sensitivity of oleic acid to pyrene ($\boldsymbol{R}_{\mathrm{OE/PY}}$) for the two components can be estimated from these plots by the equation

$$\frac{i_{264+282}}{i_{202+203}+i_{264+282}} = \frac{R_{\mathrm{OE/PY}}\chi_{\mathrm{OE}}}{1+(R_{\mathrm{OE/PY}}-1)\chi_{\mathrm{OE}}} \quad (1)$$

where i264+282 and i202+203 are the signal intensities of the main oleic acid and pyrene peaks and XOE is the mole fraction of oleic acid. The magnitude of the relative sensitivity depends on several factors:

$$R_{\mathrm{OE/PY}} = \left(\frac{\sigma_{\mathrm{OE}}}{\sigma_{\mathrm{PY}}}\right)\left(\frac{F_{\mathrm{OE}}}{F_{\mathrm{PY}}}\right)\left(\frac{S_{\mathrm{OE}}}{S_{\mathrm{PY}}}\right) \quad (2)$$

where σ is the photoionization cross section, F is the fraction of the total ion current from a compound that is observed at the molecular ion m/z, and S is the sampling efficiency. The sampling efficiency is less than 1 because of particle bounce and evaporation. Based on the data in Figure 5b, the relative sensitivity of oleic acid to pyrene is found to be greater for laser desorption (5.0) than thermal desorption (2.0). The higher relative sensitivity for oleic acid by laser desorption most likely reflects a lower sampling efficiency for pyrene owing to its greater volatility.

Baer and co-workers have used laser desorption/VUV photoionization to analyze organic compounds in single particles between about 1 and 4 µm in diameter.Typically, a spectrum is averaged over 100 particles to improve the signal-to-noise ratio and the total amount of material analyzed is on the order of 50 pg or more. This total amount of sample can be readily detected by PIAMS, although it requires on the order of 100 laser shots to desorb all collected material from the probe surface. Therefore, the shot-to-shot sensitivities of the two methods are comparable.

Source Sampling. The ability of PIAMS to distinguish common sources of ambient organic aerosol was tested by offline sampling of diesel bus exhaust, gasoline engine exhaust, meat cooking aerosol, wood burning aerosol, and cigarette smoke. For each source, replicate samples were collected in stainless steel canisters, transported to the laboratory, and analyzed within 10-15 min of sampling. Figure 6 shows the mass spectra obtained from four of these sources. alkylbenzenes that serve as octane enhancers in the fuel. This is a surprising result as these compounds should partition into the gas phase. However, several points should be kept in mind. First, the signal in this spectrum clearly comes from the condensed phasesno signal was detected if the desorption laser was blocked. Second, it is unlikely that these compounds arose simply from gas-phase condensation onto the probe surface inside the sources.

Diesel exhaust from an idling bus was sampled at a distance 0.5 m behind the exhaust pipe. A mass spectrum from this source was obtained from 50 cm^3 of aerosol (ambient temperature and pressure) from the canister. The spectrum, shown in Figure 6a, is dominated by alkyl fragments including 57, 69, 71, 81, 83, 95, 97, 109, and 111 m/z. These peaks can be attributed to unburned fuel droplets consisting of high molecular weight hydrocarbons, as observed previously with thermal desorption/electron ionization mass spectrometry. Other significant ions include 59, 63, and 75, which could correspond to nitro organics or amines. The overall signal intensity was very high and persisted for many more laser shots that the test aerosols described above, suggesting that multiple particle layers were deposited on the probe surface.

Gasoline exhaust from an automobile loaded with 93 octane gasoline was sampled in a manner similar to the bus exhaust. The car was idle with the engine not yet warm. The mass spectrum obtained from 100 cm3 of aerosol from this source, shown in Figure 6b, had a very low overall intensity as expected from the low emission levels of gasoline-powered vehicles. Lowmass ions (<80 m/z) were filtered out by the ion gate to improve detection of higher mass ions. Enhanced signal intensities were observed at 92, 106, 120, 134, and 148 m/z, which correspond to alkylbenzenes that serve as octane enhancers in the fuel. This is a surprising result as these compounds should partition into the gas phase. However, several points should be kept in mind. First, the signal in this spectrum clearly comes from the condensed phasesno signal was detected if the desorption laser was blocked. Second, it is unlikely that these compounds arose simply from gas-phase condensation onto the probe surface inside the source region. Most of the gas entering the inlet was pumped away, and as stated above, no gas-phase ionization signal was observed. Third, these compounds remained on the probe under vacuum for the duration of the measurement (over 1 min), suggestingthat they were strongly chemisorbed or even covalently bonded to the particle. Finally, we note that the detection of small aromatic species from exhaust particles shown here is similar in many respects to our previous work with coal samples, which also liberated small aromatic molecules when heated to a high temperature. It is unlikely that these compounds would be detected by conventional GC/MS analysis of the particulate emissions from this source because they would be lost during the sample preparation process.

A meat cooking aerosol was sampled above a charcoal grill. Ground beef (20% fat) was cooked for ~7 min with the aerosol sampled into the canister ~0.5 m downwind of the grill toward the end of the cooking period. The mass spectrum in Figure 6c was obtained from 100 cm^3 of the aerosol. In addition to low-m/z fragment ions indicative of aliphatic molecules, enhanced signal intensities in the high-m/z region are observed at 256 and 284 m/z, which correspond to palmitic acid and stearic acid, respectively. Palmitic acid is emitted at a rate of 481.2 mg/kg of ground beef cooked, and its ambient annual average concentration is on the order of 125 $ng/m^{3.3}$ Stearic acid is emitted at a rate of 250 mg/kg of ground beef cooked, and its ambient annual average concentration is on the order of 55 $ng/m^{3.3}$ The peak

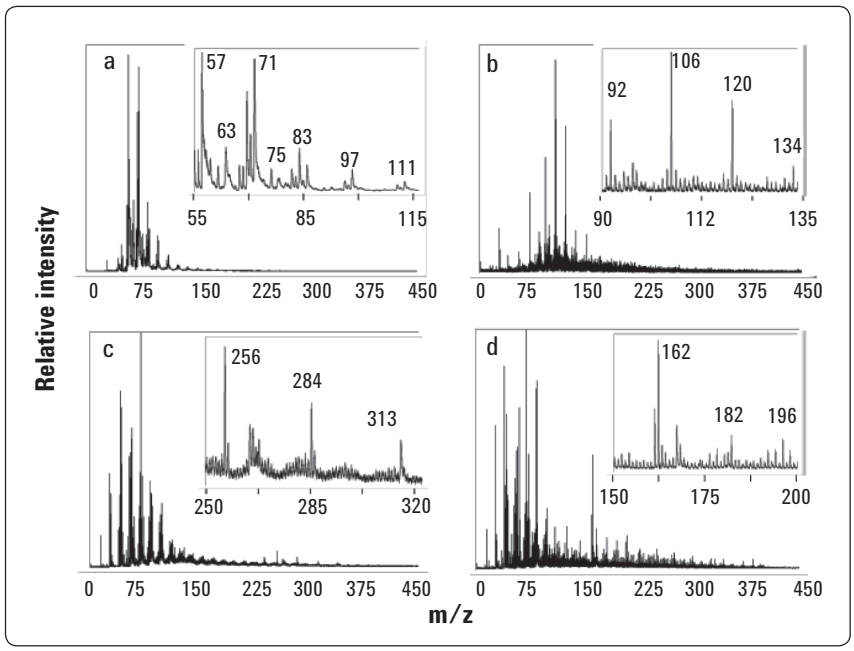

Figure 7. *PIAMS spectra for different types of ambient organic aerosol: (a) diesel engine; (b) gasoline engine; (c) meat cooking; (d) wood burning.*

at 313 m/z may be a fragment ion from cholesterol, which is an ion observed previously by Rogge et al. using 70-eV EI.40 However, no enhanced signal intensity at the molecular ion m/z is observed as would be expected from Figure 2b. The ratio of cholesterol to stearic acid in meat cooking aerosol is variable, ranging from 1:2 to 1:24. It is not known if the two are emitted evenly over the time period of cooking.

Wood smoke is a major contributor to the ambient aerosol, estimated to be on the order of 14% of the average annual fine particle emissions in Los Angeles air.53 A mass spectrum of the aerosol from a residential fireplace burning oak wood is shown in Figure 6d. An enhanced signal intensity is observed at 162 m/z, which corresponds to the molecular ion of levoglucosan (1,6-anhydro-,-D-glucopyranose), a combustion product of cellulose that is used as a molecular marker for biomass burning. Levoglucosan is emitted at a rate of 700 mg/kg of wood burned.

Cigarette smoke is estimated to be on the order of 1% of the fine particle mass concentration in Los Angeles outdoor air with a mass concentration of 0.3 Ìg/m^3. Cigarette smoke was sampled from a "light" brand cigarette, which contained a reduced level of nicotine, and mixed with makeup air to dilute the aerosol. The mass spectrum of this sample (not shown), exhibits ion current at almost every m/z, which is not uncommon for samples of vegetative burn. An enhanced signal intensity is observed at 162 m/z which corresponds to the molecular ion of nicotine. In a previous study, the most abundant compound found in cigarette smoke was nicotine with an emission rate of 1.2 mg/cigarette.

Future Directions. The photoionization aerosol mass spectrometer described in this work is capable of detecting particulatephase aliphatic and aromatic molecules in the low- to midpicogram range. The signal intensity scales linearly with sample size and is independent of particle size, permitting quantitative measurements to be made. Although molecular fragmentation is observed, particularly for aliphatic materials, the soft ionization capability of PIAMS is sufficient to distinguish major sources of ambient organic aerosol.

The ultimate goal of this work is to detect molecular ions of organic compounds in the particle phase at ambient levels. The current version of PIAMS provides detection limits in the 5-50- pg range with a 1-min sampling interval and an inlet flow rate of 0.1 L/min. Individual compounds in an aerosol can be detected at a level of 50-500 ng/m^3, which is sufficient for smog chamber studies. To detect compounds at ambient levels, the sensitivity must be increased by a factor of 100. This can be addressed in a couple of ways. First, the sampling inlet can be redesigned. Particle collection devices with air flows exceeding 10 L/min are readily available37 and could be adapted for use with PIAMS so that a sufficient amount of material is sampled during a 1-min interval. Second, the collection probe/laser desorption setup could be reconfigured. Cooling the collection probe would reduce evaporation and permit longer sampling intervals to be used. Different probe/desorption laser combinations may reduce the amount of fragmentation induced by the desorption step and thereby increase the signal-to-noise ratio of the molecular ion. Some of these changes have been implemented recently and have permitted well over a 1 order of magnitude increase in sensitivity. Therefore, the prospects are bright that PIAMS will permit highly time-resolved source apportionment of ambient aerosol based on the distribution of organic compounds.

Acknowledgment

This material is based upon work supported by the National Science Foundation under Grant CHE0098831.

Product specifications and descriptions in this document subject to change without notice.

For more information on the Acqiris product line, sales or services, see our website at:
www.agilent.com/find/acqiris

Contacts

Agilent Acqiris Product Information

USA	**(845) 782-6544**
Asia-Pacific	**61 3 9210 2890**
Europe	**41 (22) 884 32 90**

Additional Agilent Contact Information

Americas

Canada	(877) 894-4414
Latin America	305 269 7500
United States	(800) 829-4444

Asia Pacific

Australia	1 800 629 485
China	800 810 0189
Hong Kong	800 938 693
India	1 800 112 929
Japan	0120 (421) 345
Korea	080 769 0800
Malaysia	1 800 888 848
Singapore	1 800 375 8100
Taiwan	0800 047 866
Thailand	1 800 226 008

Europe and Middle East

Austria	0820 87 44 11
Belgium	32 (0) 2404 93 40
Denmark	45 70 13 15 15
Finland	358 (0) 10 855 2100
France	0825 010 700*
	*0.125 €/minute
Germany	01805 24 6333**
	**0.14 €/minute
Ireland	1890 924 204
Israel	972-3-9288-504/544
Italy	39 02 92 60 8484
Netherlands	31 (0) 20 547 2111
Spain	34 (91) 631 3300
Sweden	0200-88 22 55
Switzerland	0800 80 53 53
United Kingdom	44 (0) 118 9276201

Other European Countries:
www.agilent.com/find/contactus

Revised: October 24, 2007

www.agilent.com

Printed in USA, March 7, 2008
5989-7560EN

Agilent Technologies